

## CHAPTER IV

### RESULTS AND DISCUSSION

#### 4.1 Catalyst Characterization

As shown in Table 4.1, the surface area measurements and cell densities of all three commercial-honeycombed monolith catalysts are summarized. The surface area of platinum ceramic-honeycombed monolith catalyst becomes the lowest value of 21.3 m<sup>2</sup>/g while the greater values of 30.9 and 48.3 m<sup>2</sup>/g are for the palladium and rhodium ceramic-honeycombed monolith catalysts, respectively. The cell densities of all catalysts are almost the same. Platinum ceramic-honeycombed monolith catalyst has a cell density of 196 cells per square inch (cps) while both palladium and rhodium ceramic-honeycombed monolith catalysts have 200 cps.

**Table 4.1** Surface area measurements and cell densities of three commercial monolith catalysts used.

Type of catalyst	Surface area (m <sup>2</sup> /g)	Cell density (cells/in <sup>2</sup> )
Platinum (Pt)	21.3	196
Palladium (Pd)	30.9	200
Rhodium (Rh)	48.3	200

## 4.2 Catalyst Activity

The catalyst screening was achieved by comparing the catalytic activity over the oxidation of diethylamine in terms of light-off temperature. The CO<sub>2</sub> formation (conversion of the DEA to CO<sub>2</sub>) as a function of reaction temperature is illustrated in Fig. 4.1 for all catalysts used. As shown in this figure, Pd catalyst illustrates the lowest light-off temperature while the higher light-off temperatures are observed for Rh and Pt catalysts, respectively. The light-off temperatures and CO<sub>2</sub> formation greater than 95% for all catalysts are presented in Table 4.2. In the case of Pd monolith catalyst, which is the most active catalyst, the CO<sub>2</sub> formation becomes appreciable in the range 250 to 280 °C while CO<sub>2</sub> formation greater than 95% is obtained at about 320 °C. For Rh and Pt catalysts, destruction efficiency greater than 95% is attained at 380 and 400 °C, respectively. It can be seen that the Pd ceramic-honeycombed monolith catalyst is the most active catalyst for the catalytic combustion of diethylamine because of the lowest light-off temperature. This result agrees with the results obtained from the literature (Borgharkar and Abraham, 1994). The activity was observed in the following sequence: Pd > Rh > Pt.

**Table 4.2** Activities in terms of light-off temperatures and temperatures at 95% conversion.

Type of catalyst	Light-off temperature at 50% conversion (°C)	Temperature @ 95% conversion (°C)
Platinum (Pt)	340	400
Palladium (Pd)	290	320
Rhodium (Rh)	325	380



### 4.3 Reaction Rate Studies

The experimental runs were performed at 250, 265, and 275 °C and carried out over Pd catalysts. The effects of reactant concentration and reaction temperature on the reaction rate were shown the following results.

#### 4.3.1 Effect of Diethylamine Concentration

In each concentration of diethylamine (DEA), the oxygen concentrations were also varied. Fig. 4.2 illustrates the effect of DEA concentration on the reaction rate at 250 °C with different concentrations of oxygen. The reaction rate increases with increasing DEA concentrations. It was found that the reaction rate linearly increases up to 5,000 ppm DEA concentration and then slightly increases when exceeds this concentration level. The reaction rate with an identical amount of DEA illustrates the similar trend of all varied O<sub>2</sub> concentrations. It can be seen that the reaction mechanism did not change. The varied DEA concentrations affect to the reaction rate whereas the varied O<sub>2</sub> concentrations do not affect. This result agrees with the results obtained from the work of Spivey (1997).

#### 4.3.2 Effect of Oxygen Concentration

The effect of oxygen concentration on the reaction rate was studied in the range of 10 to 35 vol%. Three DEA concentrations were also used to examine this effect on the reaction rate when oxygen concentrations were varied. The results as shown in Fig. 4.3 indicate the independence of reaction rate on the varied oxygen concentrations between 10 to 35 vol%. As a result, this oxygen concentration range did not affect to the reaction rate because it is excess comparing to diethylamine concentration. This result agrees with the work of Spivey (1997).

### 4.3.3 Effect of Reaction Temperature

Fig. 4.4 illustrates the effect of reaction temperatures on the reaction rate at different concentrations of diethylamine. As shown in this figure, the results indicate that the reaction rates increase with increasing temperatures. In chemical kinetic region, the heat of the reaction is released on the catalyst surface and has to be transported away from the surface. If the concentration of the reactant is very low, no heat is built up in the catalyst and the reaction rate follows the Arrhenius expression. For this reason, the higher the temperatures, the greater the reaction rates. This result agrees with the theory obtained from the study of Fogler (1992).

## 4.4 Kinetic Parameter Studies

The complete kinetic analysis involving the kinetic parameters can be markedly simplified by the usage of a differential reactor. The advantages of differential reactor involve the decrease in reaction temperature and concentration gradients in the reactor. The diminution avoids complications caused by the gradients and can significantly simplify the kinetic analysis. In this work, a differential mode of operation in a tubular reactor was attained by limiting the CO<sub>2</sub> formation.

### 4.4.1 Reaction Order with respect to DEA Concentration

The effect of diethylamine concentrations on the reaction rate was investigated at 250 and 265 °C. The experiments were carried out over the Pd catalysts. Fig. 4.5 illustrates the relationship between the diethylamine oxidation rate at a given temperature and diethylamine concentration. The results showed the linear lines whose slopes are directly represented the reaction order with respect to diethylamine concentration. The reaction order was found to be 0.56 with respect to the diethylamine concentration. In

chemical kinetic regime, the reaction rate depends on the reaction temperature because the rate constant is strongly temperature-dependent. The reaction order is temperature-independent. This result agrees with the theory obtained from the study of Fogler (1992).

#### 4.4.2 Reaction Order with respect to Oxygen Concentration

For the conditions encountered in most VOC control applications, the concentration of oxygen will always be much larger than the concentration of the organic reactant. Therefore, the oxygen partial pressure will be essentially constant during the reaction. Fig. 4.6 illustrates the reaction rate as a function of oxygen concentration. According to the results shown in Fig. 4.6, the reaction rate at a given temperature was independent on the oxygen concentration because the similar slopes were obtained to be close to zero. This result agrees with the result obtained from the work of Papaethimiou *et al.* (1997).

#### 4.4.3 Apparent Activation Energies

The temperature effect on the reaction rate was studied in the temperature range of 250-400 °C. The reactions were carried out over the Pd catalysts at the atmospheric pressure. The Arrhenius plots of the reaction rate as a function of the reciprocal absolute temperature are depicted in Figs. 4.7 (a), (b), and (c) for three different regions; chemical kinetic, pore diffusion, and bulk mass transfer, respectively. These figures show the linear lines whose slopes were represented the apparent activation energies. The highest apparent activation energy in chemical kinetic region was obtained at 18.8 kcal/mole shown in Fig. 4.7(a). This result was agreed with the combustion of non-halogenated volatile organic compounds over group VIII metal catalysts. Apparent activation energies of those reactions over Pt and Pd catalysts were found to be in the range of 16.7 to 28.6 kcal/mole. This result agrees with the

results obtained from the work of Papaethimiou *et al.* (1997). The intermediate value of 9.9 kcal/mole was observed in the pore diffusion region shown in Fig. 4.7(b). Finally, the smallest apparent activation energy in bulk mass transfer region was attained at 2.2 kcal/mole shown in Fig. 4.7(c). As the results, the catalytic combustion of diethylamine over Pd ceramic-honeycombed monolith catalyst was controlled by the reaction in chemical kinetic region. This result agrees with the theory obtained from the study of Heck *et al.* (1989).

#### 4.4.4 Kinetic Model

The kinetic model of a catalytic combustion of diethylamine over the Pd catalyst was empirically established according to a power law rate equation, which expresses the rate as a product of a rate constant and the reactant concentrations raised to a power. The rate constant was dependent on the temperature and the apparent activation energy of the reaction can be determined from the Arrhenius equation as shown in Eq. (4.1)

$$r = k_0 e^{-\left[\frac{E_a}{RT}\right]} C_{\text{DEA}}^m \cdot C_{\text{O}_2}^n \quad (4.1)$$

where

$r$  = the reaction rate;

$k_0$  = the pre-exponential factor;

$E_a$  = the apparent activation energy;

$R$  = the universal gas constant, = 1.987 cal/mole;

$T$  = the absolute temperature, K;

$C_{\text{DEA}}$  and  $C_{\text{O}_2}$  = the concentrations of diethylamine and  $\text{O}_2$ , respectively;

$m$  and  $n$  = the empirically determined reaction orders of diethylamine and  $\text{O}_2$ , respectively.

$$\ln r = \ln k_o - \frac{E_a}{R} \left( \frac{1}{T} \right) + m \ln C_{DEA} + n \ln C_{O_2} \quad (4.2)$$

Because of the reaction rate at a given temperature was approximately zeroth order with respect to the oxygen concentration, the last term of Eq. (4.2) can be negligible. Then, the reaction rate as a function of reaction temperature shows the slope and intercept as the following Eqs.(4.3) and (4.4):

$$\text{Slope} = \frac{-E_a}{R} \quad (4.3)$$

$$\text{Intercept} = \ln k_o + m \ln C_{DEA} \quad (4.4)$$

According to above both equations, the kinetic parameters such as the apparent activation energy,  $E_a$ , and pre-exponential factor,  $k_o$ , can be calculated. At this present study, the kinetic model was empirically established in the chemical kinetic region. The apparent activation energy was obtained at 18.8 kcals/mole and the pre-exponential factor was determined to be 201.4.

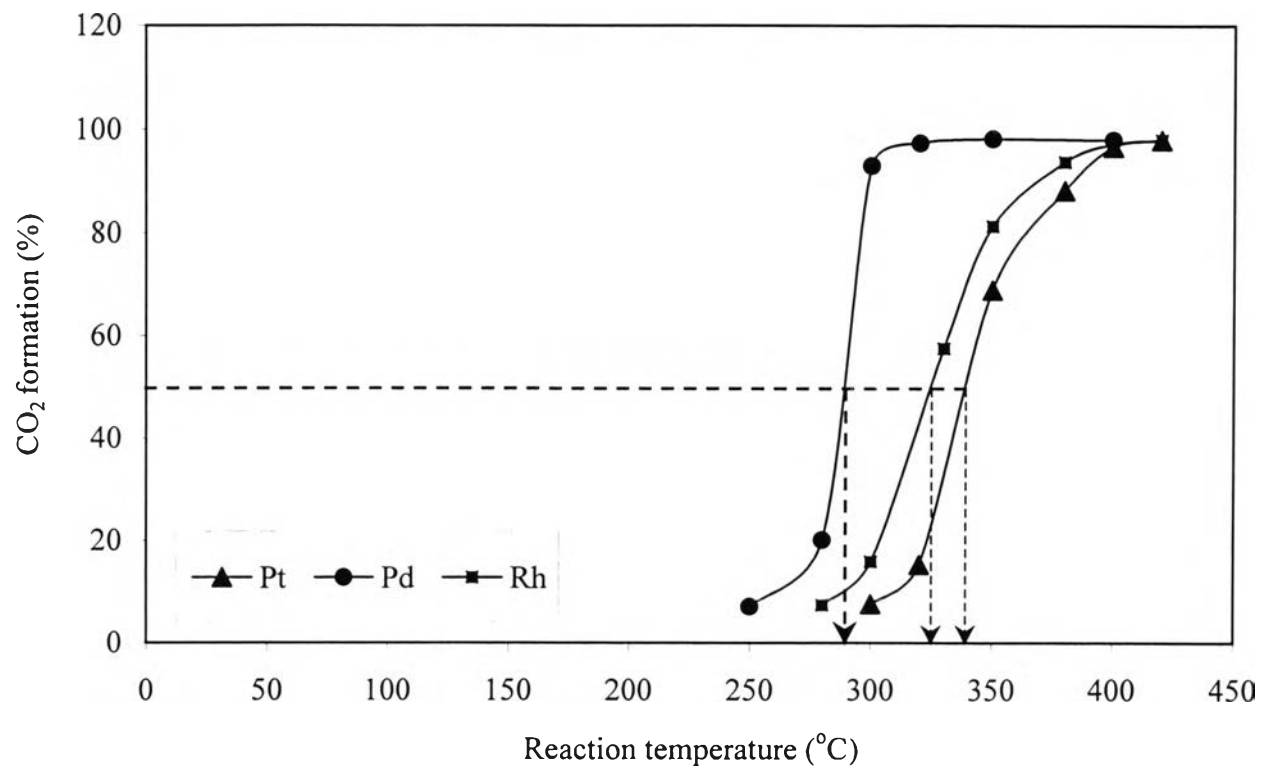


**Fig. 4.1** Catalytic activities in terms of the light-off temperatures (2,000 ppm DEA and 21 vol% O<sub>2</sub> with 18,200 GHSV).



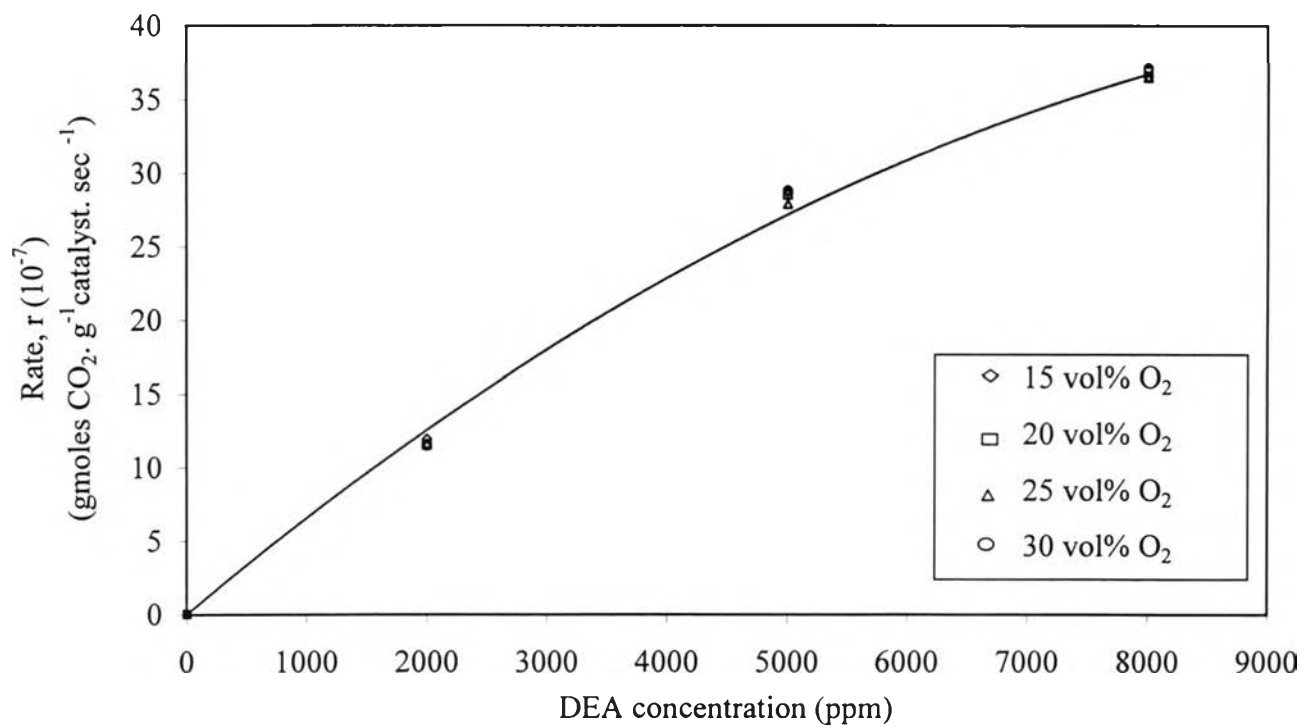


**Fig. 4.2** Effect of DEA concentrations on the reaction rate at 250°C and 18,200 GHSV with different  $\text{O}_2$  concentrations.

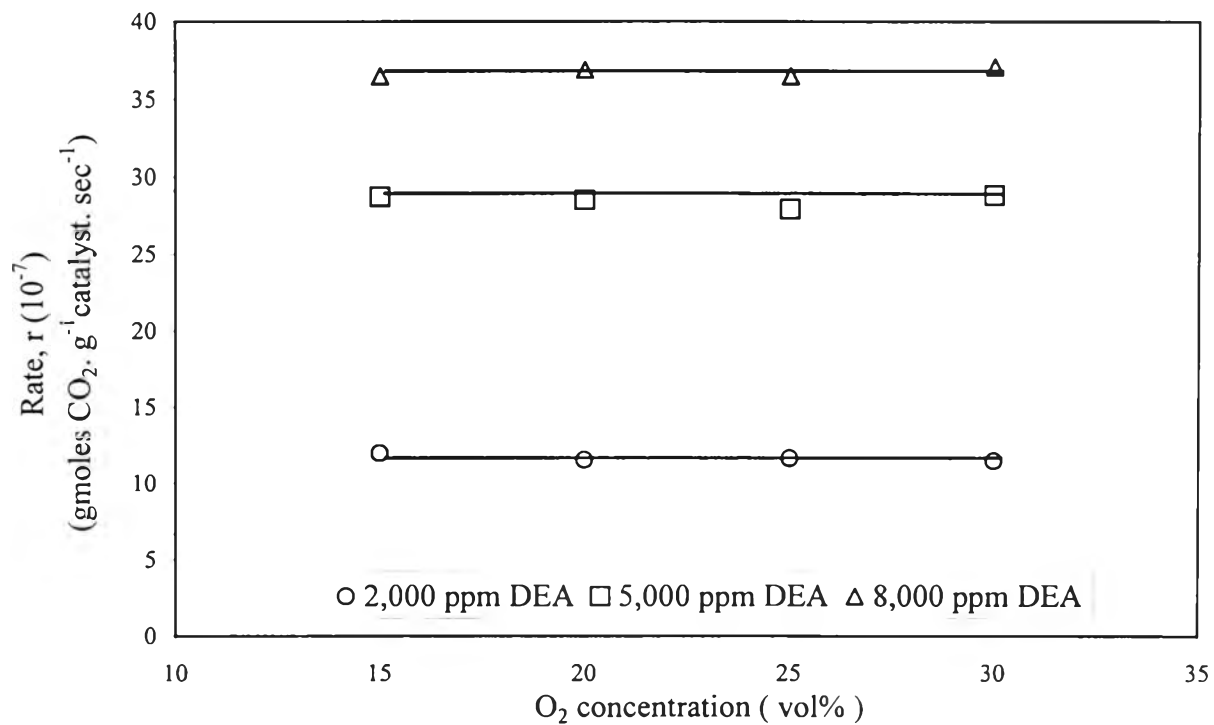
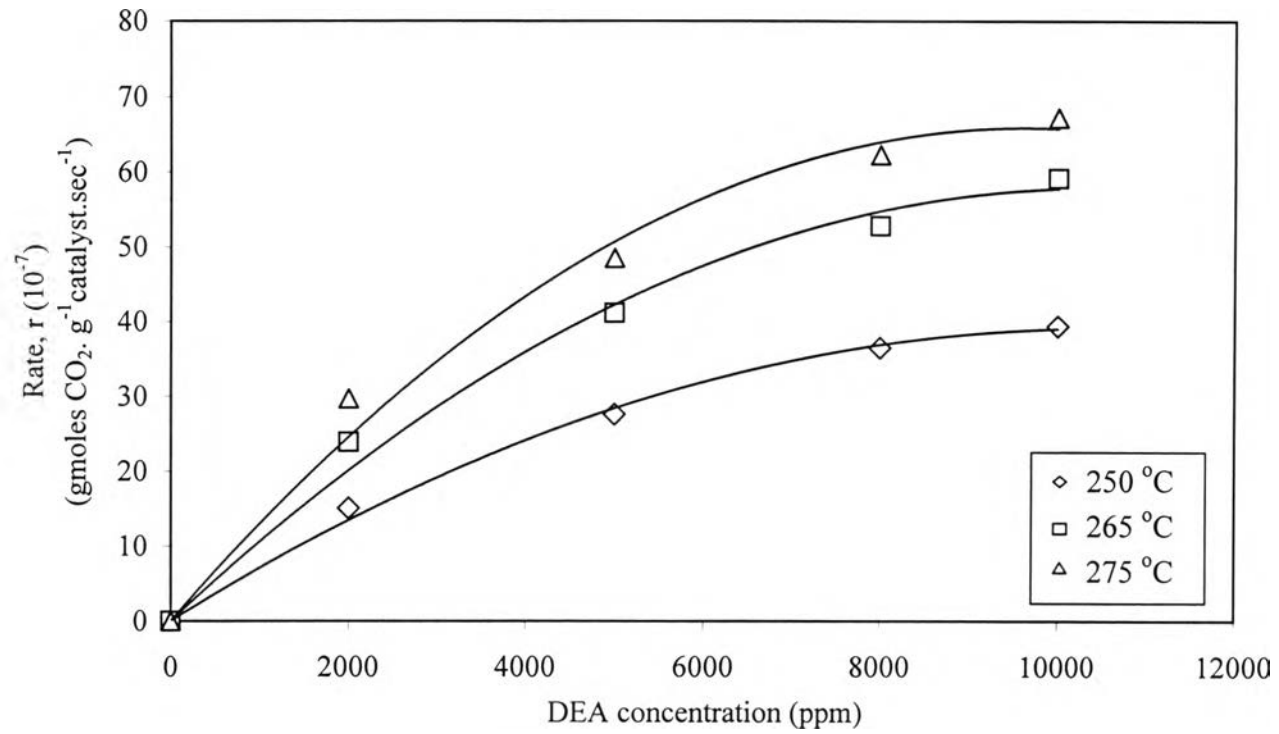
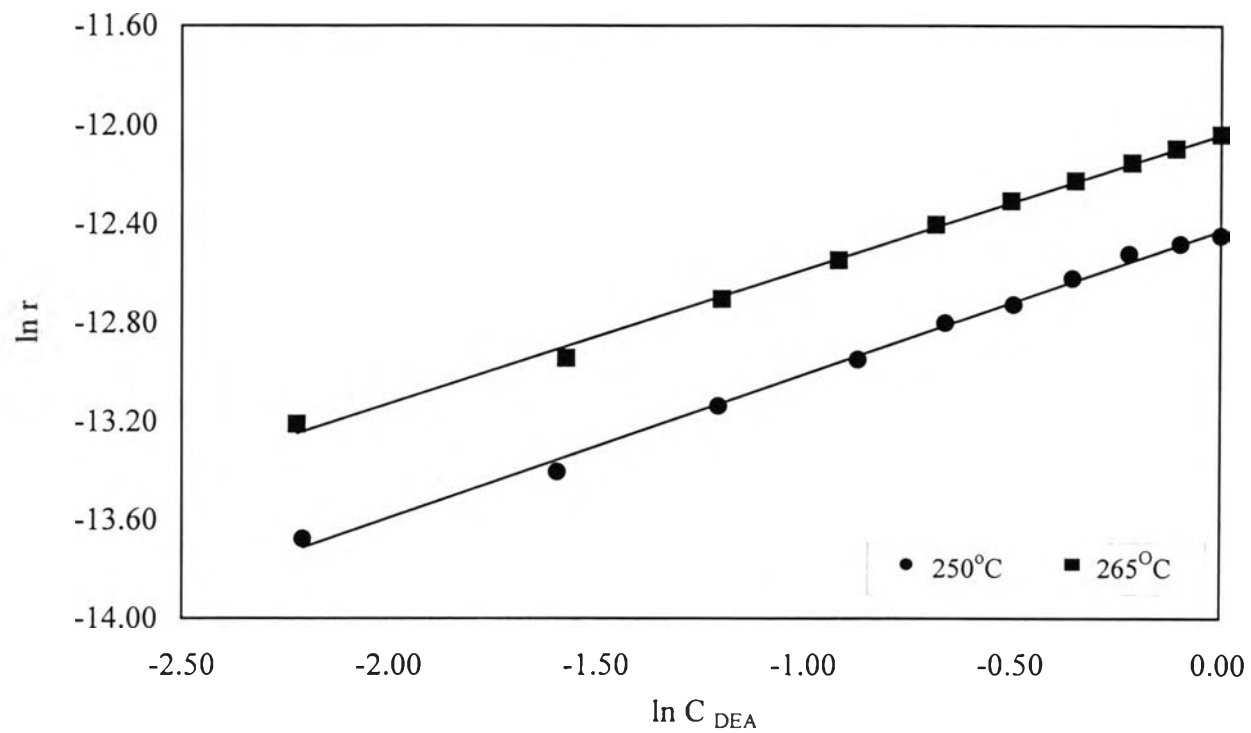


Fig. 4.3 Effect of  $\text{O}_2$  concentrations on the reaction rate at  $250^\circ\text{C}$  and 18,200 GHSV with different DEA concentrations.



**Fig. 4.4** Effect of reaction temperature on the reaction rate at different DEA concentrations (21 vol% and varied 2,000 to 10,000 ppm DEA with 18,200 GHSV).



**Fig. 4.5** Plot of the reaction rate as a function of DEA concentrations (21 vol% O<sub>2</sub> and varied 1,000 to 10,000 ppm DEA at 18,200 GHSV).

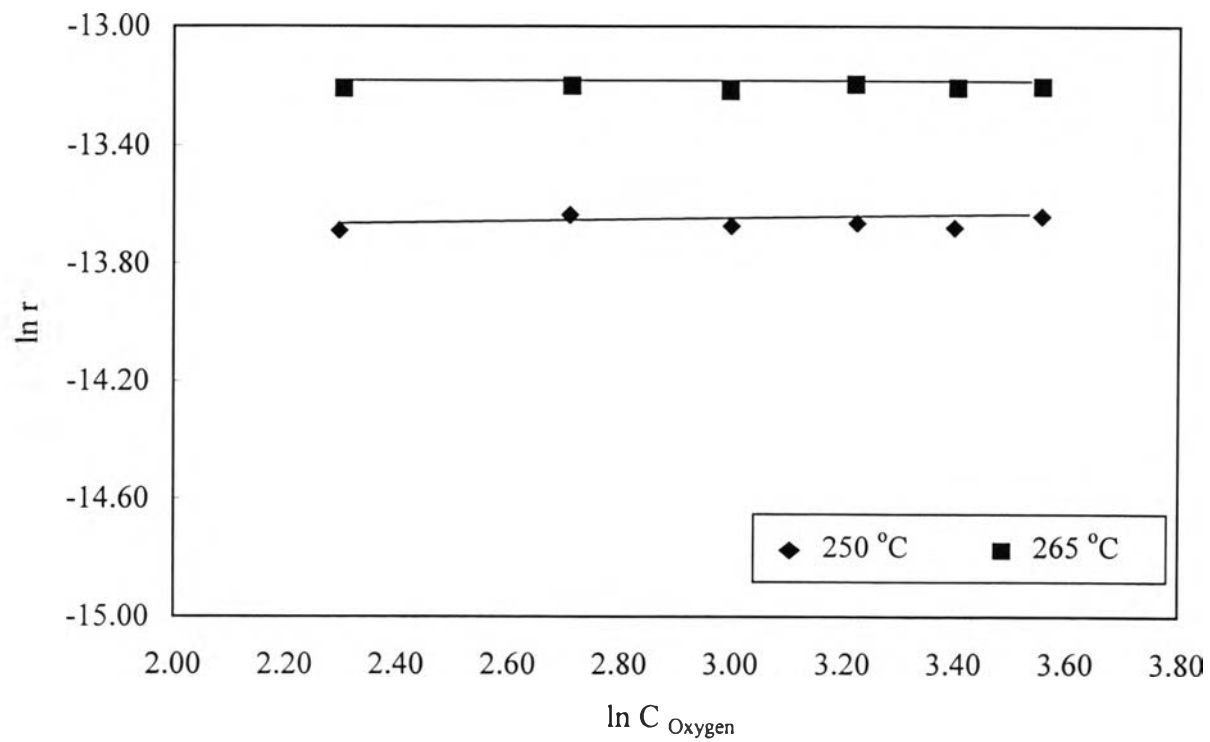


**Fig. 4.6** Plot of the reaction rate as a function of  $\text{O}_2$  concentrations (2,000 ppm DEA and varied 10-35 vol%  $\text{O}_2$  at 18,200 GHSV).

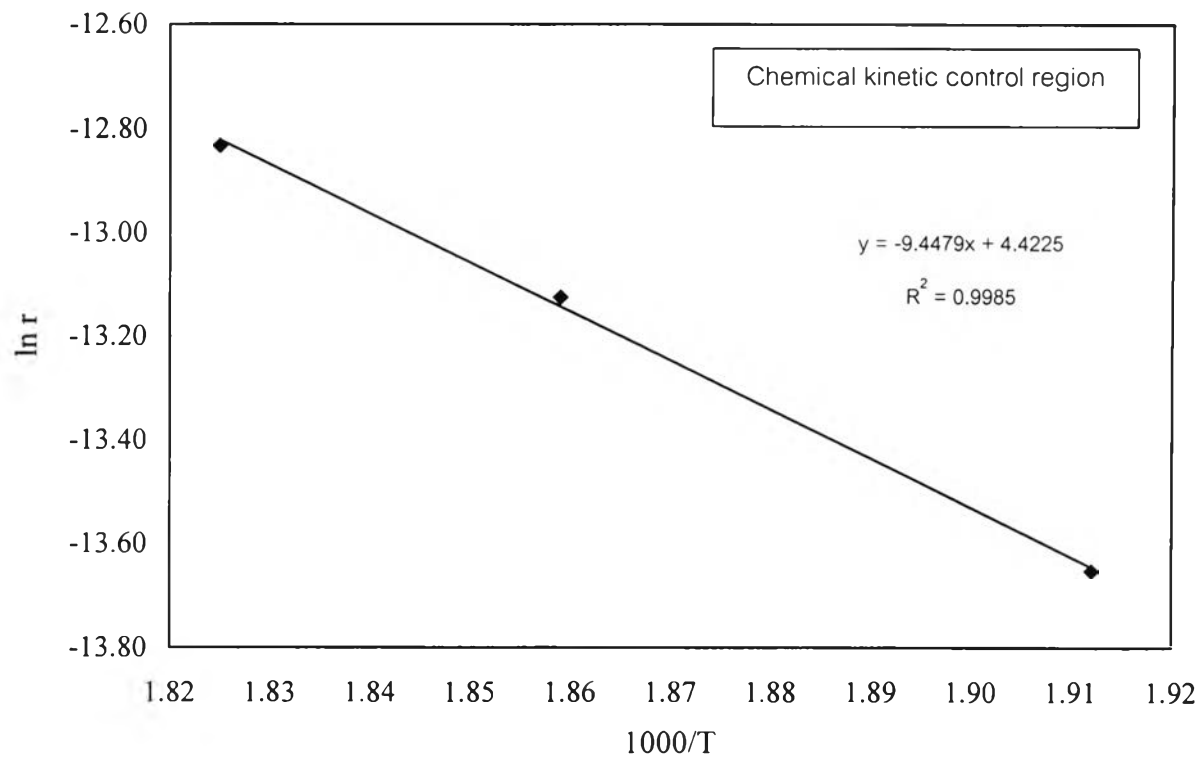


**Fig. 4.7 (a)** Arrhenius plot for determining activation energy (2,000 ppm DEA and 21 vol% O<sub>2</sub> at 18,200 GHSV).

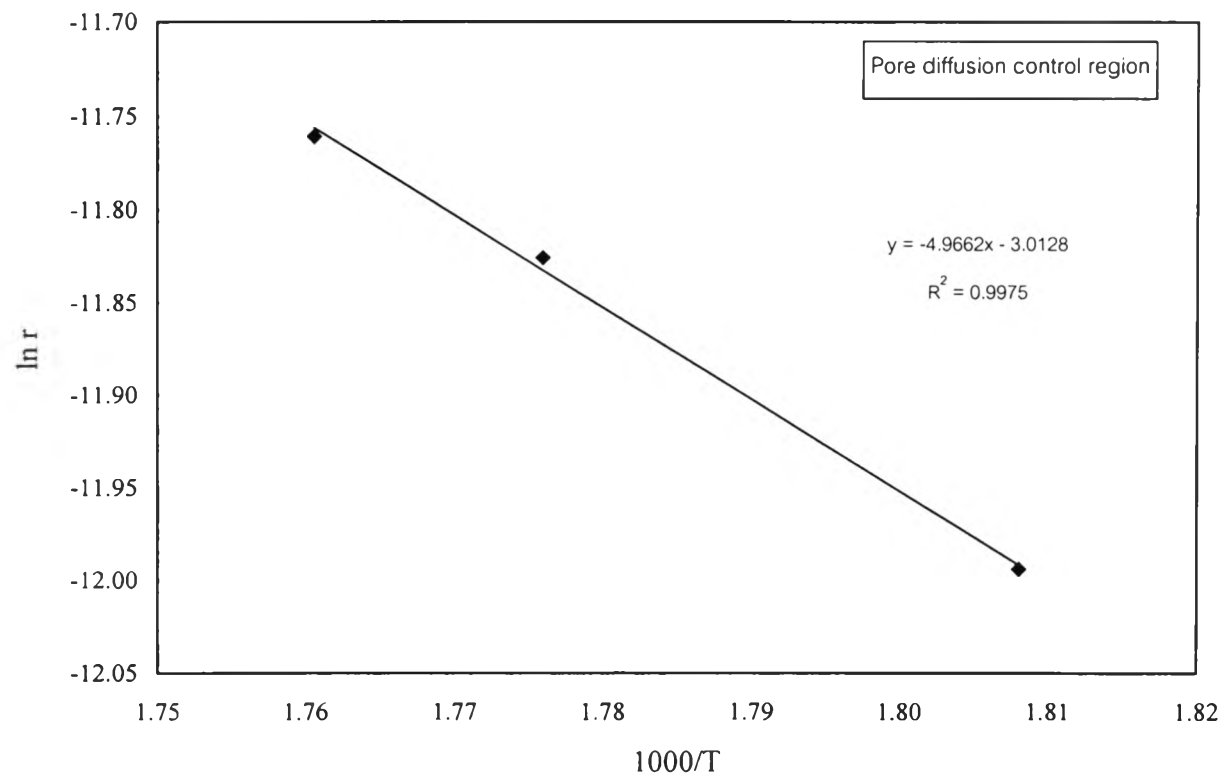


**Fig. 4.7 (b)** Arrhenius plot for determining activation energy (2,000 ppm DEA and 21 vol% O<sub>2</sub> at 18,200 GHSV).

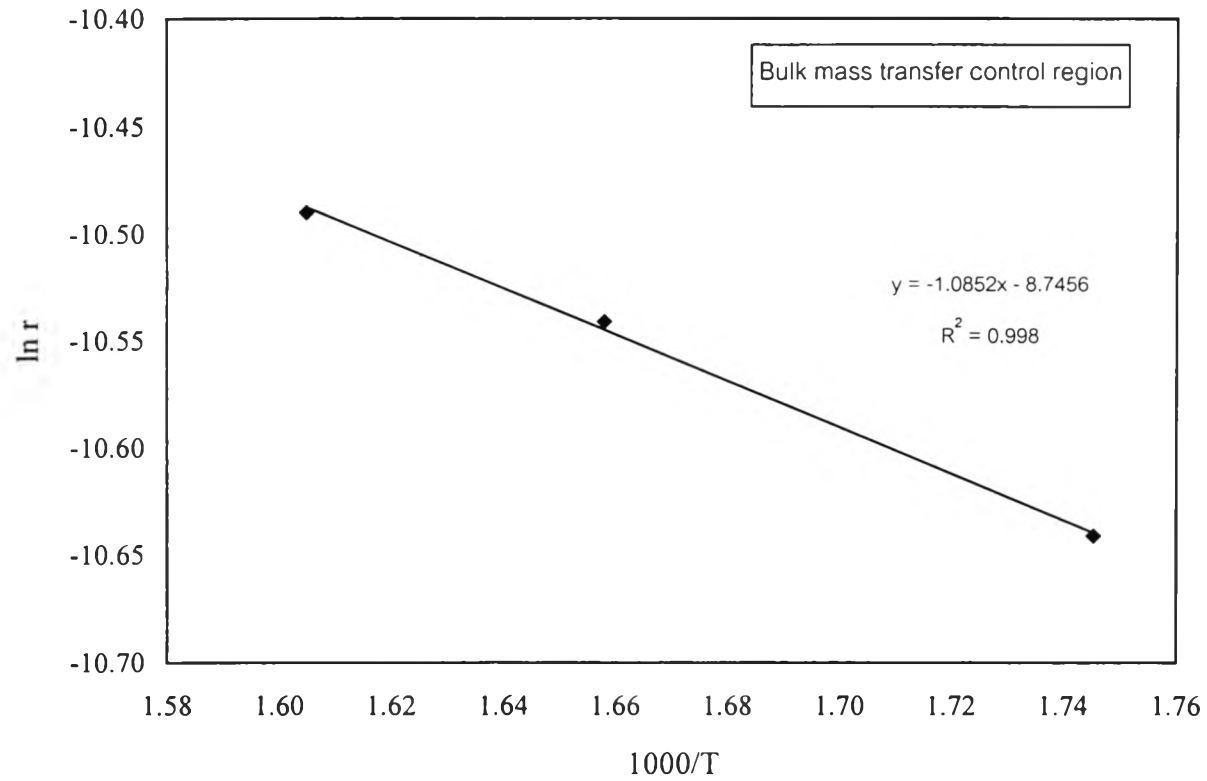


**Fig. 4.7 (c)** Arrhenius plot for determining activation energy (2,000 ppm DEA and 21 vol% O<sub>2</sub> at 18,200 GHSV).